



The Mediterranean Green Energy Forum 2013, MGEF-13

Photovoltaic glazing: analysis of thermal behavior and indoor comfort

G.M. Tina^{a*}, A.Gagliano^b, F. Nocera^b, F.Patania^b

^a Department of Electrical, Electronics and Computer Engineering, Catania University, Viale A.Doria 6, 95125 Catania, Italy

^b Energy and Environmental Division of D.I.I., Catania University, Viale A.Doria 6, 95125 Catania, Italy

Abstract

The integration of photovoltaic systems into buildings is one of the best ways to exploit effectively solar energy and to realize the distributed generation inside urban and suburban environmental. BIPV can be installed in a wide variety of applications such as skylights, roofing, walls and windows but, glazing is perhaps the most promising application. In this context the development of products with the best compromise between electrical efficiency and control of transparency will see the most competition between competing companies and those that win this battle will inevitably come to be successful in the market. Most BIPV glass today uses crystalline silicon absorber layers which are inherently opaque, whereas better transparency could be achieved at a reasonable level of efficiency using other absorber layers such as very thin layers of CIGS or dye sensitive cells.

Specifically in this research the thermal behavior of a BIPV glass product using c-Si by means of one-layer model is performed. The PV module temperature is then used to evaluate the thermal radiant field in a sample room. An application to a typical thermal comfort computation is finally presented.

© 20xx The Authors. Published by Elsevier Ltd.

Selection and peer-review under responsibility of KES International

Keywords: Type your keywords here, separated by semicolons ;

1. Introduction

The application of Photovoltaic technology in buildings has attracted worldwide attention for energy savings and environmental side-effect reductions. Photovoltaic generate electrical power by converting

* Corresponding author. Tel.: +39 095 7382337; fax: +39 095 330793.

E-mail address: gmtina@dieei.umict.it.

solar radiation into direct current electricity using semiconductors that exhibit the photovoltaic effect. Photovoltaic power generation employs solar panels composed of a number of cells containing photovoltaic material. Materials presently used for photovoltaic include mono-crystalline silicon, polycrystalline silicon, amorphous silicon, cadmium telluride, and copper indium selenide/sulfide [1]. Due to the growing demand for renewable energy sources, the manufacturing of solar cells and photovoltaic arrays has advanced considerably in recent years [2].

Nomenclature

| | |
|------------------|--------------------------------------------------------------------------|
| clo | thermal resistance of clothing |
| C | convective sensible heat loss from skin (W/m^2) |
| C_{res} | rate of convective heat loss from respiration (W/m^2) |
| d | distance of the human being from the glazing surface (m) |
| E_{res} | rate of evaporative heat loss from respiration (W/m^2) |
| E_{sk} | evaporative heat loss from the skin (W/m^2) |
| $F_{\text{p-i}}$ | view factors between a subject and internal surfaces |
| I | irradiance (W/m^2) |
| L | thermal load (W) |
| M | rate of metabolic heat production (W/m^2) |
| PMV | predicted mean vote |
| PPD | predicted percentage dissatisfied |
| q_{res} | total rate of heat loss through respiration (W/m^2) |
| q_{sk} | total rate of heat loss from skin (W/m^2) |
| R | radiative sensible heat loss from skin (W/m^2) |
| S_{cr} | rate of heat storage in core compartment (W/m^2) |
| S_{sk} | rate of heat storage in skin compartment (W/m^2) |
| S_{PV} | PV module area (m^2) |
| T_{a} | outdoor air temperature |
| T_{i} | indoor air temperature |
| T_{bg} | temperature of back glass |
| T_{fg} | temperature of front glass |
| T_{si} | temperature of surrounding surface (K) |
| T_{mr} | mean radiant temperature (K) |
| T_{PV} | operating temperature of a PV module |
| T_{sk} | skin temperature |
| V_{in} | indoor air velocity (m/s) |

| | |
|-----------|-------------------------------------|
| V_{out} | outdoor air velocity (m/s) |
| W | rate of mechanical work (W/m^2) |

BIPV are photovoltaic materials that are used to replace conventional building materials in parts of the building envelopes, such as the roofs, skylights or facades. They are increasingly incorporated into the construction of new buildings as a principal or ancillary source of electrical power, although existing buildings may be retrofitted with BIPV modules as well. The advantage of integrated photovoltaic over more common non-integrated systems is that the initial cost can be offset by reducing normal construction costs of building materials and labor for parts of the building replaced by BIPV modules. These advantages make BIPV one of the fastest growing segments of the photovoltaic industry [3].

BIPV are considered a functional part of the building structure, or they are architecturally integrated into the building's design. This category includes designs that replace the conventional roofing materials, such as shingles, tiles, slate and metal roofing. These types of products can be indistinguishable from their non-photovoltaic counterparts. Aesthetically, this can be attractive if there is a desire to maintain architectural continuity and not to attract attention to the array. BIPV modules can also be architectural elements that enhance the building's appearance and create very desirable visual effects. These types of arrays include custom-made module sizes and shapes with opaque or transparent spaces between the cells and can be used for curtain walls, awnings, windows and skylights [4,5].

The results of studies on the temperature and generation performance of photovoltaic modules have been reported by some researchers [6–8]. Building designers are faced with many challenges in solar housing design. Integration of PV panels into buildings is more than simply connecting electrical and building envelope components. The PV panels should be integrated appropriately to maximize the use of solar energy and increase cost effectiveness [9]. For BIPV systems to achieve multifunctional roles, various factors must be taken into account, such as the photovoltaic module temperature, shading, installation angle and orientation. Among these factors, the irradiance and photovoltaic module temperature should be regarded as the most important factors because they affect: the electrical efficiency of the BIPV system, the energy performance and the thermal comfort of buildings where BIPV systems are installed. Occupants situated near windows often experience thermal discomfort. In the summer, glazing interior temperatures are usually higher than indoor air temperature, often causing discomfort due to high radiant temperature asymmetry and increased operative temperature. In addition, solar radiation falling directly on the occupant can exacerbate discomfort. In order to quantify thermal comfort in a perimeter zone, the thermal environment must be evaluated including climatic conditions, indoor air temperature, mean radiant temperature and radiant temperature asymmetry, in addition to defining other environmental and personal parameters [10]. Transient two-node thermal comfort model have been utilized to considered the variability of the external climatic conditions [11]. To define the thermal comfort conditions of a climate it must be given some characteristic parameters of the environment and its occupants. Six primary factors identified to most affect the thermal comfort are air temperature, humidity, air velocity, mean radiant temperature, clothing level and metabolic rate.

2. Thermal and energetic model of PV window

The operating temperature of a PV module, T_{PV} , represents a variable which affects its efficiency, greatly for c-Si technology less for thin film technology. Therefore evaluating module thermal behavior from prevailing meteorological conditions becomes not only an essential task in devising energy production capacities but also, specifically, to calculate the impact of PV glazing on internal thermal comfort. In literature there are many methods to calculate the module temperature, such as: energy balance [6], where there is a parameter that is empirically determined, depending by wind speeds; temperature measurements

on the back of PV module [12], an expression is used to evaluate the cell temperature, this equation depends also by the wind and by some empirical parameters; “mounting coefficient” [13], used in order to estimate the cell temperature for situations other than the original free-standing case. The most known method is based on the knowledge of NOCT (Normal Operating Cell Temperature), that is given by the PV modules manufacturers. But this method does not take into account the real ventilation of PV modules, especially if the PV modules are building integrated. Further classification of thermal model is based on number of layers in which the PV module is divided, that is: single layer [14-16], one equation is used in order to calculate the PV module temperature, multi-layer [17, 18] a PV panel is divided into several horizontal sections, thus a thermal balance equation is written for each layer.

In this paper a five layer thermal model is used [19], as it is able to precisely estimate the operating temperatures of the PV layers in real outdoor operating conditions, especially when the ambient conditions on the front face of the PV module are different from the back ones. Further considering that in this case the PV module is glass to glass type the width of the back cover is not negligible in the T_{PV} calculation. The entire ensemble of a PV module encased in glass consists of five mediums: glass, resin, silicon, resin and glass. However, as the optical and thermal properties of glass and resin are almost identical and the thickness of the resin is very small, only three mediums must be considered, glass, silicon and glass. The following three isothermal regions are considered (see Fig. 1.a): front (glass), central (silicon) and the rear one (glass). A thermal equivalent electrical circuit can be used effectively to find the thermal fluxes and the unknown temperatures in a PV module. Fig. 2.b shows an equivalent circuit related to a five-layer model [19]. It is worth noticing that the voltage source T_{sky} is a voltage controlled voltage source as it depends on the ambient temperature T_a .

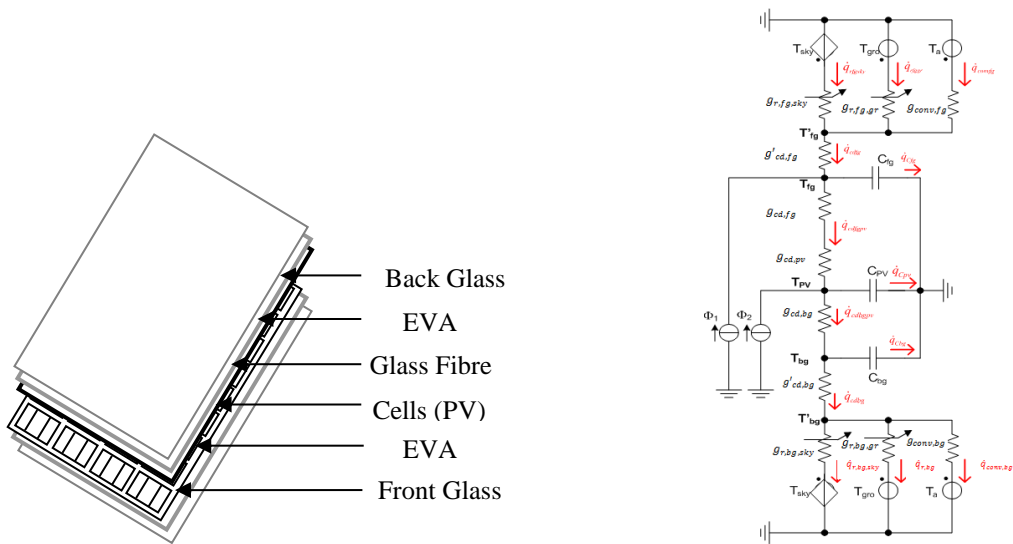


Fig. 1. PV module: a) layers and b) equivalent thermal circuit for a five layer model [19];

3. Thermal comfort model

In the context of thermal comfort the Fanger [20] theory is the most commonly adopted. It is based on thermoregulation and heat balance equations. According to this theory, the human body employs

physiological processes in order to maintain a balance between the heat produced by metabolism and the heat lost from the body. The comfort equation describes thermal comfort as the imbalance between the actual heat flow from the body, in a given thermal environment, and the heat flow required for optimum comfort (i.e. neutral), for a given activity. Fanger proposed the condition for thermal comfort that is obtained when the skin temperature and sweat secretion lie within narrow limits. To evaluate the thermal indoor comfort, it is worth remembering that a human being does not feel the room temperature, he feels the heat loss from the body. The environmental parameters that must be measured are those which affect the energy loss, namely: air temperature (T_i), mean radiant temperature (MRT), air velocity (v_{in}) and humidity (HR). The influence of these parameters on energy loss is not equal and it is not sufficient to measure only one of them [21]. To deduce the comfort equation, it was combined the comfortable temperature of the skin and the sweat production equation with the full body thermal balance [22]. An expression for optimal thermal comfort can be deduced from the metabolic rate, clothing insulation and environmental conditions, as follows:

$$M - W = (C + R + E_{sk}) + (C_{res} + E_{res}) + (S_{sk} + S_{cr}) \quad (1)$$

Equation (1) contains three physiological variables; the heat loss by evaporation of sweats (E_{sk}), skin temperature (T_{sk}) that is included in the $C+R$ terms and metabolic rate (M). Equ. (1) also describes the relationship between measurements of physical parameters and thermal sensation experienced by a person in an indoor environment. The comfort equation is an operational tool where physical parameters, combined with the metabolic heat generated by human activity and clothing worn by a person, can be used to assess the thermal comfort conditions of an indoor environment.

3.1. Predicted mean vote equation

The thermal comfort equation is only applicable to a person in thermal equilibrium with the environment. However, the equation only gives information on how to reach optimal thermal comfort by combining the variables involved. Therefore, it is not directly suitable to ascertain the thermal sensation of a person in an arbitrary climate where these variables may not satisfy the equation. Fanger used the heat balance equation to predict a value for the degree of sensation using his own experimental data and other published data for any combination of activity level, clothing value and the four thermal environmental parameters.

The predicted mean vote (PMV) is the mean vote expected to arise from averaging the thermal sensation vote of a large group of people in a given environment. PMV is a mathematical expression involving activity, clothing and the four environmental parameters, expressed by eqn(2)

$$PMV = 3.155 \cdot (0.30 \cdot e^{-0.114 \cdot M} + 0.28) \cdot L \quad (2)$$

Where L is the thermal load on the body, defined as the difference between internal heat production and heat loss to the actual environment.

Equation 2 relates thermal conditions to the seven-point ASHRAE thermal sensation scale. PMV scale is constituted by seven thermal sensation points ranging from -3 (cold) to +3 (hot), where 0 represents the neutral thermal sensation. The ASHRAE standard specifies the conditions where a fraction of the occupants find the environment thermally acceptable.

Fanger also developed a related index, called the predicted percentage dissatisfied (PPD):

$$PPD = 100 - 95 \cdot e^{(0.03353 \cdot PMV^4 + 0.2179 \cdot PMV^2)} \quad (3)$$

This index is calculated from PMV and, it predicts the percentage of people who are likely to be dissatisfied with a given thermal environment.

ISO 7730 and ISO 7726 show new PMV and PPD calculating methods, these technical standards provide a classification of environments depending on the degree of thermal comfort, further they add a new concept, named adaptation, which can be used to assess facilities and indoor environments.

3.2. Mean radiant temperature

The mean radiant temperature of an environment is defined as the uniform temperature of an imaginary black enclosure in which an occupant would exchange the same amount of radiant heat as in the actual nonuniform space[23].

$$T_{mr}^4 = \sum_i T_{si}^4 \cdot F_{p-i} \quad (4)$$

The calculation methods derive the mean radiant temperature from the knowledge of the absolute surface temperature of the surrounding surfaces (i), T_{si} , and the view factors between the person and the surrounding surfaces, F_{p-i} . The view factors between a seated or standing subject and the internal surfaces have been documented by Fanger and developed into charts. For simulation purposes; however, this method proves inadequate since the view factors can only be determined visually from the charts. The algorithm developed by Cannistraro [24] was used to calculate the view factors between a subject and internal surfaces, F_{p-i} . The angle factor between the person and a rectangular surface is computed as a function of width, a, and height, b, of the surface and as a function of the distance, c, between the person and the surface, by means of the following equation:

$$F_{p-i} = F_{max} \cdot \left[1 - e^{-\left(\frac{a}{c}\right)/\tau} \right] \left[1 - e^{-\left(\frac{a}{c}\right)/\gamma} \right] \quad (5)$$

where

$$\tau = A + B \left(\frac{a}{c} \right) \quad (6)$$

$$\gamma = C + D(b/c) + E(a/c) \quad (7)$$

The coefficients F_{max} , A, B, C, D and E assume different values for seated or standing postures of the person, for known or unknown orientation of the person with respect to surrounding surfaces and for vertical or horizontal surface.

Using Eqs. (5), (6) and (7) the following equation of the mean radiant temperature can be obtained:

$$T_{mr} = \sqrt[4]{\sum_{i=1}^6 F_{max} \left\{ \left\{ 1 - \exp \left[-\frac{a/c}{\tau} \right] \right\} \left\{ 1 - \exp \left[-\frac{b/c}{\gamma} \right] \right\} T_i^4 \right\}} \quad (8)$$

If a person is seated near a glazing exposed to solar radiation (beam and diffuse), the calculation of MRT becomes more complex since it needs to take into account not only effect of the highest temperature of the interior surfaces, but also the components of solar radiation striking a person. An

algorithm to calculate the MRT of an indoor space under these circumstances has been developed by La Gennusa et al. [25] .

4. Numerical simulation and performance evaluation

The experimental data of a double glass PV module, where mono crystalline solar cells two sheets of glass with space left between the cells to allow light to shine through, are used. The encapsulation of cells is made between two sheets of tempered glass with high transmittance. The dimension of the module is 1042 mmx462 mm x45mm. It has been selected as a typical sample to analyse the performance of PV window systems. Fig. 2 shows main ambient variables (irradiance, I , ambient temperature T_a and wind speed, V_{out}) normalized by their respective maximum values, that mainly affect the operating PV module temperature. The numerical analysis has been limited to the diurnal hours from 6:00 am and 18:00 pm. The temperatures reported in fig 3 refer to a crystalline silicon PV module, the width of both front and back glass is 4 mm, further the 75% of the module is covered by PV cells. The module is installed vertically and it is assumed that is working at maximum power point and its efficiency at standard test conditions (STC) is 13% with a thermal maximum power coefficient of 0.0044 ($1/C^\circ$). The highest T_{PV} temperature in fig. 3 is about 45 °C, at the following conditions: $I=900 \text{ W/m}^2$, $T_a= 24 \text{ }^\circ\text{C}$ and $V_{out}=1 \text{ m/s}$. This calculated temperature is credible, as the module is working at conditions very close to the NOCT conditions ($I=800 \text{ W/m}^2$, $T_a= 25 \text{ }^\circ\text{C}$ and $V_{out}=1 \text{ m/s}$, open circuit) and the NOCT temperature is 42 °C.

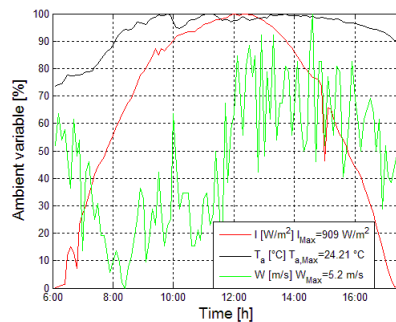


Fig. 2. Normalized ambient variable

The considered model is one-dimensional one, as it is made of a serial assembling of one-dimensional elementary models, which explains the essential thermal transfers. In fact, for each layer just one temperature is assigned, so distribution of the temperature along the three dimensions of the module is neglected. In this paper the distribution of the temperature along the surface of the module has not been considered. In [26] for a frameless PV module it has been found that temperature field is not uniform but it has a maximum in center and the minimum along the border, the difference is about five degree.

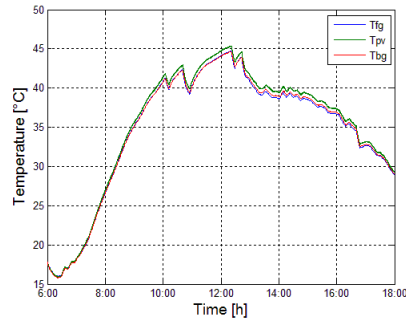


Fig. 3. Diurnal PV module layer temperatures: T_{fg} (front glass), T_{pv} (PV cells), T_{bg} (back glass)

4.1. Analysis of indoor thermal comfort

For evaluating thermal comfort in perimeter zones in a given environment with an highly-glazed PV façade, mathematical simulations were carried out. In the simulations a BIPV window of variable surface, placed in a test chamber of 4x4x3 meters, is considered. The MRT was calculated from the equation 8, using the algorithms implemented in Matcad environment. The internal environment was considered at a constant temperature, $T_i = 26\text{ °C}$, whereas the surface temperatures of inner walls are equal to $T_{si} = 299\text{ K}$, finally the temperature of the photovoltaic glass surface, T_{pv} , was calculated by the numerical simulations previously described and, then, fixed at 318 K. Three sizes of the photovoltaic window, S_{pv} , were considered, whose values normalized respect with the floor surface (16 m^2) are: 0.5, 0.25 and 0.125. Figure 4 shows, for a grid step of 0.5 m, the view factor and the variation of MRT in the room for a person sitting in front of the PV window.

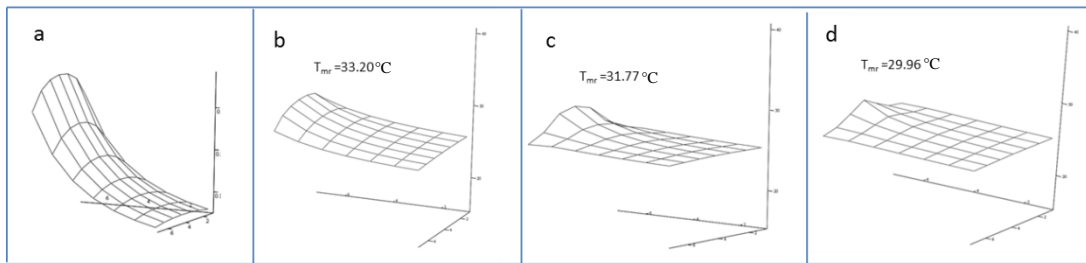


Fig. 4. Distribution of heat radiative parameters inside the room: a) View factor; b) T_{mr} for $S_{pv} = 8.00\text{ m}^2$; c) T_{mr} for $S_{pv} = 4.00\text{ m}^2$; d) T_{mr} for $S_{pv} = 2.00\text{ m}^2$.

Based on the calculated MRT, the PMV was evaluated at distances from the glazing surface, d , of 0.5 m and 2.0 m. Environmental and personal variables used in the comfort model are: $M = 70\text{ W/m}^2$; $RH = 55\%$; $V_{int} = 0, 1\text{ m/s}$; $clo = 0.75$ ($0.115\text{ m}^2\text{K/W}$). Table 1 report the comfort indexes calculated for the different cases.

Table 1. Comfort indexes

| | $S_{pv}=8.0 \text{ m}^2$ | | $S_{pv}=4.0 \text{ m}^2$ | | $S_{pv}=2.0 \text{ m}^2$ | |
|---------|--------------------------|--------|--------------------------|--------|--------------------------|--------|
| | d=0.5m | d=2.0m | d=0.5m | d=2.0m | d=0.5m | d=2.0m |
| MRT(°C) | 33.20 | 28.41 | 31.77 | 27.46 | 29.96 | 26.81 |
| PMV | 1.63 | 1.01 | 1.44 | 0.89 | 1.21 | 0.80 |
| PPD | 58.71 | 26.67 | 43.88 | 21.83 | 35.90 | 18.93 |

The predicted thermal sensation corresponds to a slightly unacceptability but acceptable conditions. Although these conditions are predicted to be physiologically “acceptable”, for the purpose of an occupant in an office building it may be uncomfortable since it is within the sweating regulation zone. Future developing of this work has to consider the effect of solar radiation and radiant temperature asymmetry (RTA).

Obviously these extreme conditions happens just for limited period of time, during the highest values of incident solar radiations.

5. Conclusions

In this paper a five layer thermal model is used, as it is able to precisely estimate the operating temperatures of the PV layers in real outdoor operating conditions, especially when the ambient conditions on the front face of the PV module are different from the back ones. The temperature calculated by PV thermal model is useful to evaluate the thermal environment in a perimeter zone near a highly-glazed surface. The comfort simulation model is being fine-tuned and generalized in order to be able to evaluate comfort conditions for typical office spaces equipped with PV window. The results indicate a very unacceptable thermal discomfort condition especially for a distance from the PV surface less than 0.5 m, with PMV values that exceed 1.5 (warm sensation) and with a very high percentage of dissatisfied more than 58 %. The thermal field is quite acceptable at distance greater than 2.0 m from the PV surface, where PMV max of about 1,0 were predicted (slightly warm).

Eventually, this model will help provide recommendations for components of high-performance facades in order to reduce or eliminate perimeter heating as a secondary source of heating in perimeter zones.

References

- [1] Jacobson MZ. Review of solutions to global warming, air pollution and energy security. *Energy & Environmental Science*, 2009; 2: 148–173.
- [2] Solangi KH, Islam MR, Saidur R, Rahim NA, Fayaz H. A review on global solar energy policy. *Renewable and Sustainable Energy Reviews*, 2011;15 :2149–2163.
- [3] Park KE, Kang GH, Kim HI, Yu GJ, Kim JT. Analysis of thermal and electrical performance of semi-transparent photovoltaic (PV) module. *Energy*, 2010;35 : 2681–2687.
- [4] Barkaszi SF, Dunlop JP. Discussion of strategies for mounting photovoltaic arrays on rooftops. *Pr.of Solar Forum*, 2001.
- [5] Crawford RH, Treloar GJ, Fuller RJ, Bazilian M. Life-cycle energy analysis of building integrated photovoltaic systems (BiPVs) with heat recovery unit. *Renewable and Sustainable Energy Reviews* 2006;10 : 559–575.
- [6] Mattei M, Notton G, Cristofari C, Muselli M, Poggi P. Calculation of the polycrystalline PV module temperature using a simple method of energy balance, *Renewable Energy* 2006;31 :553–567.
- [7] Carr AJ, Pryor TL. A comparison of the performance of different PV module types in temperate climates. *Solar Energy* 2004;76 : 285–294.
- [8] Chenni R, Makhoul M, Kerbache T, Bouzid A. A detailed modeling method for photovoltaic cells, *Energy*,32 : 1724–1730.
- [9] Gagliano A, Patania F, Nocera F, Capizzi A, Galesi A. GIS-based decision support for solar photovoltaic planning in urban environment. *International Conference on Sustainability in Energy and Buildings 2012*.
- [10] Bessoudo M, Tzempelikos A, Athienitis A, Zmeureanu R. Simulation of thermal comfort conditions in highly-glazed perimeter zones with shading devices. *2nd Canadian Solar Buildings Conference 2007*.
- [11] Zmeureanu R, Doramajian A. Thermally Acceptable Temperature Drifts Can Reduce the Energy Consumption for Cooling in Office Buildings. *Building and Environment* 1992; 27: 469-481.
- [12] King DL, Boyson E, Kratochvi JA. Photovoltaic array performance model. Sandia National Lab., New Mexico 2004.
- [13] Skoplaki E, Boudouvis A, Palyvos J. A simple correlation for the operating temperature of photovoltaic modules of arbitrary mounting. *Solar Energy Materials & Solar Cells*, 2008; 1393-1402
- [14] Matsukawa H, Kurokawa K. Temperature Fluctuation Analysis of Photovoltaic Modules at Short Time Interval. *Photovoltaic Specialists Conference*, Thirty-first IEEE 2005; 1816 - 1819
- [15] Wei T, Yiping W. Effect of urban climate on building integrated photovoltaics performance. *Energy Conversion & Management*, 2007; 48: 1-8
- [16] Cueto JD. Model for thermal characteristic of flat-palte photovoltaic modules deployed at fixed tilt. 28th PVSC, IEEE2000; 1441 - 1445
- [17] Notton G, Cristofari C, Mattei M, Poggi P. Modelling of a double-glass photovoltaic module using finite differences. *Applied Thermal Engineering*, 2005; 25: 2854-2877
- [18] Wong PW, et al. Field Study and Modelling of Semi-transparent PV in power, Thermal and Optical Aspects. *JAABE* 2005;4: 549-556.
- [19] Tina GM, Marletta G, et al. Multi-layer thermal models of PV modules for monitoring applications, *38th PVSC IEEE*, 2012.
- [20] Fanger PO. *Thermal comfort*. McGrawHill, New York 1972.
- [21] Patania F, Gagliano A, Nocera F, Galesi A. Thermal Comfort in operating room: a case study. *WIT Transactions on Biomedicine and Health*, 15, pp. 105-114.
- [22] Stanton N, Brookhuis K, Hedge A, Salas E, Hendrick HW. *Handbook of Human Factors and Ergonomics Methods*. CRC Press, 2005
- [23] ASHRAE *Handbook – Fundamentals*, Chapter 8. Atlanta: ASHRAE, Inc., 2005.
- [24] Cannistraro G, Franzitta G, Giaconia C. Algorithms for the calculation of the view factors between human body and rectangular surfaces in parallelepiped environment. *Energy and Building* 1992; 19
- [25] La Gennusa M, Nucara A, Rizzo G, Scaccianocce G. The calculation of the mean radiant temperature of a subject exposed to the solar radiation—a generalised algorithm. *Building and Environment* 2005;40: 367–375
- [26] Tina G, Abate R. Experimental verification of thermal behaviour of photovoltaic modules. IEEE, 2008. MELECON.